Supplementary Information for

Rod Particle-Like Viscoelastic Behavior of Hydroxypropylmethyl Cellulose Samples with Narrow Molar Mass Distributions Dissolved in Aqueous solutions

Misato Yoshida[1], *Daiki Nakagawa*[1], *Kengo Arai*[1], *Yoshiki Horikawa*[1,2] *and Toshiyuki Shikata*[1,2*]

[1]Cellulose Research Unit, Tokyo University of Agriculture and Technology, 3-5-8 Saiwai-cho, Fuchu, Tokyo 183-8509, Japan

[2]Division of Natural Resources and Eco-materials, Graduate School of Agriculture, Tokyo University of Agriculture and Technology, 3-5-8 Saiwai-cho, Fuchu, Tokyo 183-8509, Japan

Introduction

In this Supplementary Information, fundamental viscoelastic parameters such as the zero-shear viscosity (η_0), the average relaxation time (τ_w) and the reciprocal steady state compliance (J_e^{-1}) determined in the flow or terminal region observed in aqueous solutions of the unfractionated original HpMC sample are concisely summarized as functions of a parameter ($\bar{L}^3\nu$), where $\bar{L}$ and ν mean the average rod particle length and the molecular number density calculated from the sample concentration (c) and the Avogadro constant (N_A) as $\nu = cN_\mathrm{A}/M_\mathrm{w}$, respectively, using the values of $\bar{L} = 210$ nm and $M_\mathrm{w} = 280$ kg mol^{-1} seen in Table 1 of the original manuscript.

Viscoelastic Data Analysis Based on the Rod Particle Concept

In the main manuscript, the viscoelastic behaviors observed in aqueous solutions of fractionated HpMC samples with narrow molar mass distributions have been mainly discussed in a low frequency range belonging to the flow or terminal region, which is controlled by the slow relaxation modes of the particles formed by the fractionated HpMC sample molecules. Because the shape of particles formed by the fractionated HpMC samples in aqueous solution has been confirmed to be a rod-like shape with the periodically twisting interior,[SI1] the obtained viscoelastic data were analyzed based on the concept of

rod particles suspension rheology in the main manuscript. The original HpMC sample molecules without fractionation would have rod-like shape and a rather broad rod particle length distribution. Therefore, the concept of the rod particle suspension rheology[SI2,SI3] was also applied to analyze the viscoelastic behaviors observed in aqueous solutions of the original HpMC sample with a broad molar mass distribution with the value of $M_w/M_n = 3.7$.

The intrinsic viscosity ($[\eta]$) of rod particles with L and d dispersed in a liquid medium was theoretically calculated and given by Eq. SI1.[SI2,SI4]

$$[\eta] = \frac{2}{45M_w}\frac{\pi N_A L^3}{\ln(L/d)+C_\eta} \quad \text{(SI1)}$$

C_η in Eq. SI1 means the contribution of hydrodynamic interactions and is estimated to be −0.93 for long rod-shaped particles with $L >> d$.[SI4] In the case of rod particles with broad L distributions, parameters L and d in Eq. SI1 should be simply replaced by the average values $\bar{L}$ and $\bar{d}$.

Because the zero-shear viscosity (η_0) can be theoretically calculated as described in the main manuscript in detail, the reduced specific viscosity defined as $\eta_{sp}N_A L^3(M_w[\eta])^{-1}$, where the specific viscosity, η_{sp}, is defied to be $\eta_0\eta_w^{-1} - 1$, is calculated for monodisperse rod particle suspensions with L as follows.[SI5,SI6]

$$\frac{N_A L^3}{M_w[\eta]}\eta_{sp} = L^3\nu\left\{1 + \frac{L^3\nu}{\alpha} + \frac{(L^3\nu)^2}{\beta}\right\} \quad \text{(SI2)}$$

Eq. SI2 is composed of the linear, squared, and cubed $L^3\nu$ terms. The squared, $(L^3\nu)^2$, term described with a constant α means the contribution of interparticle interactions and corresponds to the Huggins constant[SI7], which is widely accepted to describe η_{sp} data quantitatively for various kinds of polymer sample solutions. Although the $(L^3\nu)^2$ term was not considered in the original Doi and Edwards (D-E) theory for rod particle suspensions, the presence of this term in the analysis of practical experimental data would be more natural.[SI6] Eq. SI2 clearly predicts that the cubed $(L^3\nu)^3$ term is an important controlling parameter for rod particle suspension rheology in the fully entangled regime. In the case of rod particle suspensions with broad L distribution, L should be simply replaced by $\bar{L}$ in Eq. SI2.

According to the D-E theory[SI2,SI3] for rod particle suspensions, viscoelastic behaviors in a moderately c or ν range are controlled by the rotational relaxation time (τ_r) of rod particles, which is described by a function of $L^3\nu$ and becomes considerably

longer than τ_{r0} with increasing $L^3\nu$.[SI2,SI3] The reduced rotational relaxation time defined as τ_r/τ_{r0} is expressed in terms of the linear and the squared $(L^3\nu)^2$ term for monodisperse rod particle suspensions as given by Eq. SI3.

$$\frac{\tau_r}{\tau_{r0}} = \frac{4N_A k_B T \tau_r}{5[\eta]\eta_w M_w} = 1 + \frac{L^3\nu}{\alpha} + \frac{(L^3\nu)^2}{\beta} \quad \text{(SI3)}$$

Because the observed average relaxation time, τ_w, corresponds to τ_r in the case of the monodisperse rod particle suspensions, Eqs. SI2 and SI3 can be applied to the viscoelastic data of aqueous solutions of the fractionated HpMC samples with the relatively small M_w/M_n values as reported in the main manuscript. However, in the case of the suspensions of broad particle length distributions, replacing L by $\bar{L}$ and τ_r by $\bar{\tau}_r$ ($= 4N_A\tau_w(3\nu J_e[\eta]\eta_m M_w)^{-1}$) is necessary to correct Eq. SI3, and finally Eq. SI4 is obtanied.[56]

$$\frac{\bar{\tau}_r}{\tau_{r0}} = \frac{4N_A\tau_w}{3\nu J_e[\eta]\eta_w M_w} = 1 + \frac{\bar{L}^3\nu}{\alpha} + \frac{(\bar{L}^3\nu)^2}{\beta} \quad \text{(SI4)}$$

The dependence of $\eta_{sp}N_A\bar{L}^3(M_w[\eta])^{-1}$ on $\bar{L}^3\nu$ obtained for aqueous solutions of the original HpMC samples are shown in Figure SI1a, and those of the $\frac{\tau_w}{\tau_{r0}}$ and $\frac{\bar{\tau}_r}{\tau_{r0}}$ data on $\bar{L}^3\nu$ in Figure SI1b. Because the $\eta_{sp}N_A\bar{L}^3(M_w[\eta])^{-1}$ data seem to follow a line with a slope of 1 in the low $\bar{L}^3\nu$ range and 3 in the high $\bar{L}^3\nu$ range as shown in Figure SI1a, the data are reasonably described with Eq. SI2. This $\bar{L}^3\nu$ dependence of $\eta_{sp}N_A\bar{L}^3(M_w[\eta])^{-1}$ is characteristic of rod particle suspensions including the fully entangled concentration regime. The solid line seen in Figure SI1a represents the theoretical model calculation using Eq. SI2 obtained assuming $\alpha = 70$ and $\beta = 500$. Because the value of α is directly related to the Huggins constant, k_H, in the manner $\alpha = L^3N_A(k_H M_w[\eta])^{-1}$, the value of $\alpha = 70$

was automatically evaluated using the determined value of $k_H = 0.65$. The value of $\beta = 500$? was adjusted to fit the calculated line to the experimental data in the $\bar{L}^3\nu > 30$ range. These α and β values are slightly different from the values for the fractionated HpMC samples reported in the original manuscript because of the difference in the molar mass distributions. Because the fractionated HpMC samples possess molar mass distributions rather narrower than the original HpMC sample, the difference in the molar mass distribution would be one of the essential reasons for the observed difference in the α and β values. When the used chemically modified water-soluble cellulose samples possess similar molar mass distributions each other, a difference in the molecular characteristics,

such as a difference in chemical species of substituted groups, would contribute to the interparticle and entanglement interactions described by α and β, respectively.

The difference between the τ_w/τ_{r0} and $\bar{\tau}_r/\tau_{r0}$ data at the same $\bar{L}^3\nu$ values is rather significant for the original HpMC as seen in Figure SI1b. The ration of the τ_w/τ_{r0} to $\bar{\tau}_r/\tau_{r0}$ data at the same $\bar{L}^3\nu$ value is evaluated to be ~5 because of the broad molar mass distributions with the M_w/M_n = 3.7 for the original HpMC sample. Here, we should discuss the dependence of the $\bar{\tau}_r/\tau_{r0}$ data on $\bar{L}^3\nu$ for aqueous solutions of the fractionated HpMC samples. The slope of all the $\bar{\tau}_r/\tau_{r0}$ data in the $\bar{L}^3\nu > 30$ range are approximately evaluated to be 2 as seen in Figure SI1b, which is the typical characteristic of rod particle suspensions in the fully entangled range[SI2,SI3]. The agreement between the experimental $\bar{\tau}_r/\tau_{r0}$ data and the lines calculated via Eq.SI4 assuming the same parameters, $\alpha = 70$ and $\beta = 500$, as used in Figure SI1a is fair. From these considerations, we might conclude that the viscoelastic behaviors observed in aqueous solutions of the original HpMC samples in the flow or terminal region are essentially controlled by the parameter $\bar{L}^3\nu$ as predicted by the rheological concept of rod particle suspensions. Especially, the effects of entanglements between the rod particles to viscoelastic behavior observed in the range of $\bar{L}^3\nu > 30$ is well described with the squared $(\bar{L}^3\nu)^2$ term as predicted by the D-E theory[SI2,SI3].

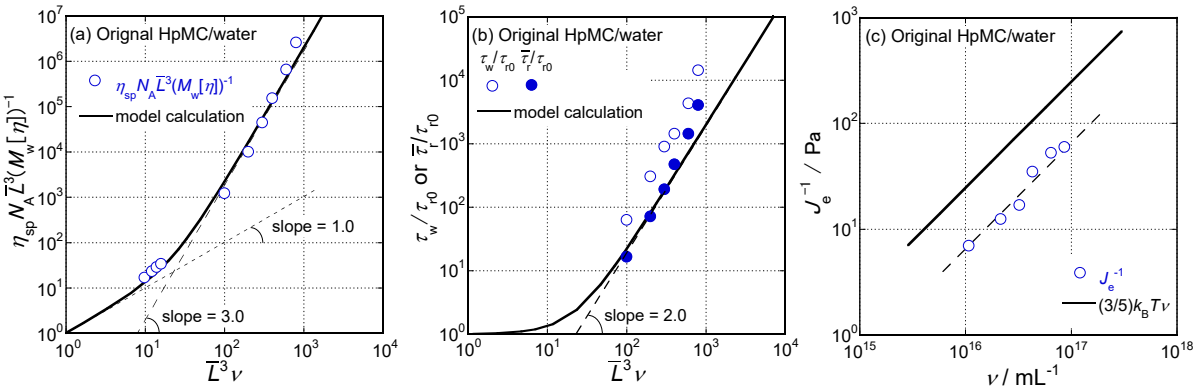

Figure SI1. Dependencies of $\eta_{sp}N_A\bar{L}^3(M_w[\eta])^{-1}$ on $\bar{L}^3\nu$ (a); τ_w/τ_{r0} and $\bar{\tau}_r/\tau_{r0}$ on $\bar{L}^3\nu$ (b); and J_e^{-1} on ν (c) for aqueous solutions of the unfractionated original HpMC samples. The solid lines in (a) and (b) demonstrate the model curves calculated with Eqs. SI2 and SI4, respectively, assuming $\alpha = 70$ and $\beta = 500$. The solid and broken straight lines in (c) represent the theoretically predicted model, $J_e^{-1} = (3/5)k_BT\nu$, for the

rod particle suspensions and an approximated ν dependence for the data described to be $J_e^{-1} = 0.15 k_B T \nu$, respectively.

Figure SI1c shows a double-logarithmic scale plot of the ν dependence of the J_e^{-1} data for aqueous solutions of the original HpMC sample. The J_e^{-1} data seem to have a slope of unity in the plot and is reasonably approximated by a broken line showing the relationship $J_e^{-1} = 0.15 k_B T \nu$. Therefore, the observed average proportional constant is substantially smaller than theoretical proportional constant of $(3/5)k_B T$[SI2,SI3]. Similar small proportional constants such as $\sim 0.2 k_B T$ were also observed in aqueous solutions of hydroxypropyl cellulose (HpC) and methyl cellulose (MC) samples with broad molar mass distributions.[SI8,SI9] Consequently, the broad molar mass distributions of the original HpMC sample molecules resulted in the observed smaller proportional constant.

In conclusion, the viscoelastic behaviors observed in aqueous solutions of the unfractionated original HpMC sample are essentially described by the concept of rod particle suspensions. The parameters such as α and β necessary to describe the viscoelastic characteristics are affected by the molar mass distribution.

Data Used in Figures

All the data used in figures shown in the main manuscript and also this Supplementary Information are tabulated below for data availability.

Table SI1. Data for **Figure 1** in the main manuscript for the aqueous HpMC(310) solution at c = 0.02 g mL^{-1}

T = 25 °C (T_{std}), a_T = 1.0					T = 10 °C, a_T = 2.1			
ω/rad s^{-1}	ωa_T/rad s^{-1}	G'/Pa	G''/Pa	η'/Pa s	ωa_T/rad s^{-1}	G'/Pa	G''/Pa	η'/Pa s (T_{std})
397								
250					525	99.1	220	0.419
158	158	43.5	110	0.696	332	89.7	159	0.479
99.7	99.7	30.0	77.4	0.776	209	65.1	120	0.573
62.9	62.9	16.6	54.6	0.868	132	40.8	90.3	0.684
39.7	39.7	9.25	37.9	0.955	83.4	24.6	66.1	0.793
25.1	25.1	4.88	25.7	1.02	52.7	14.0	46.9	0.890

15.8	15.8	2.53	17.0	1.08	33.2	7.55	32.2	0.970
9.98	9.98	1.25	11.1	1.11	21.0	3.84	21.6	1.03
6.30	6.30	0.623	7.13	1.13	13.2	1.88	14.2	1.07
3.97	3.97	0.309	4.57	1.15	8.34	0.868	9.22	1.11
2.51	2.51	0.168	2.92	1.16	5.27	0.412	5.92	1.12
1.58	1.58	0.110	1.86	1.18	3.32	0.209	3.78	1.14
0.999	0.999	0.0773	1.19	1.19	2.10	0.112	2.41	1.15
0.630	0.630	0.0598	0.766	1.22	1.32	0.0701	1.54	1.16
0.398	0.398	0.0498	0.492	1.24	0.836	0.0496	0.976	1.17
0.251	0.251	0.0408	0.319	1.27	0.527	0.0367	0.622	1.18
0.158	0.158	0.0337	0.208	1.32	0.332	0.0275	0.398	1.20
0.100	0.0999	0.0275	0.137	1.37	0.210	0.0202	0.255	1.21

T = 0 °C, a_T = 3.6					T = −5 °C, a_T = 4.9			
ω/rad s^{-1}	ωa_T/rad s^{-1}	G'/Pa	G''/Pa	η'/Pa s (T_{std})	ωa_T/rad s^{-1}	G'/Pa	G''/Pa	η'/Pa s (T_{std})
397					1950	184	412	0.212
250	900	166	259	0.288	1220	222	279	0.228
158	569	146	200	0.352	774	189	222	0.287
99.7	359	109	159	0.443	489	141	181	0.370
62.9	226	73.0	125	0.552	308	97.5	146	0.474
39.7	143	46.8	95.4	0.668	195	64.4	114	0.586
25.1	90.4	28.4	70.5	0.780	123	40.3	86.2	0.701
15.8	56.9	16.2	50.3	0.884	77.4	23.8	63.0	0.814
9.98	35.9	8.73	34.8	0.969	48.9	13.3	44.5	0.910
6.30	22.7	4.46	23.5	1.04	30.9	7.02	30.5	0.988
3.97	14.3	2.16	15.5	1.08	19.5	3.52	20.4	1.05
2.51	9.04	1.02	10.1	1.12	12.3	1.69	13.4	1.09
1.58	5.69	0.482	6.48	1.14	7.74	0.805	8.69	1.12
0.999	3.60	0.230	4.15	1.15	4.90	0.383	5.58	1.14
0.630	2.27	0.118	2.64	1.16	3.09	0.181	3.56	1.15
0.398	1.43	0.0672	1.67	1.17	1.95	0.100	2.26	1.16
0.251	0.904	0.0438	1.06	1.17	1.23	0.0577	1.43	1.16
0.158	0.569	0.0318	0.676	1.19	0.774	0.0372	0.908	1.17

0.100	0.360	0.0246	0.431	1.20		0.490	0.0290	0.578	1.18

Table SI2. Data for **Figure 2** in the main manuscript for the fractionated HpMC(310) sample

T/°C	T^{-1}/K^{-1}	ln a_T (c = 0.02 g mL^{-1})	c/g mL^{-1}	E^*/kJ mol^{-1}
35	3.25×10^{-3}	-4.31×10^{-1}	2.00×10^{-3}	24.31
25	3.35×10^{-3}	0.00	5.00×10^{-3}	29.06
10	3.53×10^{-3}	7.42×10^{-1}	1.00×10^{-2}	34.32
0	3.66×10^{-3}	1.28	1.50×10^{-2}	35.10
−5	3.73×10^{-3}	1.59	2.00×10^{-2}	34.66
			3.50×10^{-2}	34.78

Table SI3. Data for **Figure 3** in the main manuscript for the fractionated HpMC samples

sample	c/g mL^{-1}	$[\eta]c$	$L^3\nu$	E^*/kJ mol^{-1}
	2.00×10^{-3}	1.02	2.35×10^{1}	2.221×10^{1}
	5.00×10^{-3}	2.54	5.87×10^{1}	2.751×10^{1}
HpMC(210)	1.00×10^{-2}	5.08	1.17×10^{2}	3.221×10^{1}
	2.00×10^{-2}	1.02×10^{1}	2.35×10^{2}	3.450×10^{1}
	3.00×10^{-2}	1.52×10^{1}	3.53×10^{2}	3.450×10^{1}
	4.00×10^{-2}	2.03×10^{1}	4.70×10^{2}	3.432×10^{1}
	2.00×10^{-3}	1.16	3.11×10^{1}	2.431×10^{1}
	5.00×10^{-3}	2.90	7.77×10^{1}	2.906×10^{1}
HpMC(310)	1.00×10^{-2}	5.80	1.55×10^{2}	3.432×10^{1}
	1.50×10^{-2}	8.70	2.33×10^{2}	3.510×10^{1}
	2.00×10^{-2}	1.16×10^{1}	3.11×10^{2}	34.66×10^{1}
	3.50×10^{-2}	2.03×10^{1}	5.44×10^{2}	34.87×10^{2}
	2.00×10^{-3}	1.56	3.78×10^{1}	2.556×10^{1}

	5.00×10^{-3}	3.90	9.46×10^{1}	3.192×10^{1}
	8.00×10^{-3}	6.24	1.51×10^{2}	3.445×10^{1}
HpMC(440)	1.20×10^{-2}	9.36	2.27×10^{2}	3.565×10^{1}
	1.70×10^{-2}	1.33×10^{1}	3.22×10^{2}	3.553×10^{1}
	2.00×10^{-2}	1.56×10^{1}	3.78×10^{2}	3.494×10^{1}
	2.75×10^{-2}	2.15×10^{1}	5.20×10^{2}	3.451×10^{1}
	3.50×10^{-2}	2.73×10^{1}	6.62×10^{2}	3.451×10^{1}

Table SI4. Data for **Figure 4** in the main manuscript for the fractionated HpMC samples

sample	$[\eta]c$	η_{sp}	$M_w(cN_Ak_BTJ_e)^{-1}$	$\tau_w(M_w[\eta])^{-1}$/mol s mL^{-1}
	1.02×10^{-1}	1.10×10^{-1}		
	1.78×10^{-1}	2.04×10^{-1}		
	2.54×10^{-1}	3.05×10^{-1}		
	3.07×10^{-1}	3.76×10^{-1}		
	3.56×10^{-1}	4.44×10^{-1}		
	3.56×10^{-1}	4.53×10^{-1}		
HpMC(210)	4.04×10^{-1}	5.16×10^{-1}		
	4.57×10^{-1}	6.21×10^{-1}		
	1.02	2.26		
	2.54	1.25×10^{1}	4.24×10^{-1}	3.75×10^{-12}
	5.08	6.64×10^{1}	3.22×10^{-1}	1.41×10^{-11}
	1.02×10^{1}	6.51×10^{2}	3.60×10^{-1}	6.56×10^{-11}
	1.52×10^{1}	2.81×10^{3}	3.39×10^{-1}	1.87×10^{-10}
	2.03×10^{1}	8.20×10^{4}	4.03×10^{-1}	3.56×10^{-10}
	1.16×10^{-1}	1.27×10^{-1}		
	1.74×10^{-1}	2.24×10^{-1}		
	2.03×10^{-1}	2.44×10^{-1}		
	2.90×10^{-1}	3.67×10^{-1}		
	3.48×10^{-1}	5.10×10^{-1}		
	4.06×10^{-1}	5.55×10^{-1}		
HpMC(310)	5.22×10^{-1}	8.22×10^{-1}		

	6.96×10^{-1}	1.25		
	1.16	3.04		
	2.90	1.81×10^{1}	4.01×10^{-1}	5.56×10^{-12}
	5.80	1.23×10^{2}	3.50×10^{-1}	2.22×10^{-11}
	8.70	4.93×10^{2}	4.42×10^{-1}	4.45×10^{-11}
	1.16×10^{1}	1.35×10^{3}	3.75×10^{-1}	1.11×10^{-10}
	2.03×10^{1}	1.36×10^{4}	4.29×10^{-1}	5.56×10^{-10}
	1.56×10^{-1}	2.01×10^{-1}		
	2.73×10^{-1}	3.66×10^{-1}		
	3.90×10^{-1}	5.64×10^{-1}		
	5.07×10^{-1}	8.00×10^{-1}		
	1.56	5.74		
HpMC(440)	3.90	4.74×10^{1}	5.33×10^{-1}	8.16×10^{-12}
	6.24	2.23×10^{2}	5.33×10^{-1}	2.33×10^{-11}
	9.36	1.01×10^{3}	5.48×10^{-1}	6.70×10^{-11}
	1.33×10^{1}	4.04×10^{3}	5.22×10^{-1}	1.95×10^{-10}
	1.56×10^{1}	7.41×10^{3}	5.95×10^{-1}	2.91×10^{-10}
	2.15×10^{1}	2.70×10^{4}	6.46×10^{-1}	6.99×10^{-10}
	2.73×10^{1}	7.11×10^{4}	6.09×10^{-1}	1.46×10^{-9}

Table SI5. Data for **Figure 5** in the main manuscript for the fractionated HpMC samples

sample	$L^3\nu$	$\eta_{sp}N_A L^3(M_w[\eta])^{-1}$	τ_w/τ_{r0}	$\bar{\tau}_r/\tau_{r0}$	ν/mL	J_e^{-1}/ Pa
	2.35	2.53				
	4.11	4.72				
	5.87	7.05				
	7.09	8.69				
	8.22	1.03×10^{1}				
	8.22	1.05×10^{1}				
HpMC(210)	9.35	1.19×10^{1}				
	1.06×10^{1}	1.43×10^{1}				
	2.35×10^{1}	5.22×10^{1}				

	5.87×10^{1}	2.89×10^{2}	8.34	5.90	1.43×10^{16}	2.00×10^{1}
	1.17×10^{2}	1.54×10^{3}	3.13×10^{1}	1.88×10^{1}	2.87×10^{16}	3.50×10^{1}
	2.35×10^{2}	1.50×10^{4}	1.46×10^{2}	8.77×10^{1}	5.73×10^{16}	8.00×10^{1}
	3.52×10^{2}	6.49×10^{4}	4.17×10^{2}	2.36×10^{2}	8.60×10^{16}	1.10×10^{2}
	4.70×10^{2}	1.90×10^{5}	7.93×10^{2}	5.32×10^{2}	1.15×10^{17}	1.70×10^{2}
	3.11	3.40				
	4.66	6.00				
	5.44	6.54				
	7.77	9.82				
	9.32	1.37×10^{1}				
	1.09×10^{1}	1.49×10^{1}				
HpMC(310)	1.40×10^{1}	2.20×10^{1}				
	1.86×10^{1}	3.34×10^{1}				
	3.11×10^{1}	8.16×10^{1}				
	7.77×10^{1}	4.85×10^{2}	8.41	5.62	9.71×10^{15}	1.60×10^{1}
	1.55×10^{2}	3.28×10^{3}	3.37×10^{1}	1.97×10^{1}	1.94×10^{16}	2.80×10^{1}
	2.33×10^{2}	1.32×10^{4}	6.73×10^{1}	4.96×10^{1}	2.91×10^{16}	5.30×10^{1}
	3.11×10^{2}	3.61×10^{4}	1.68×10^{2}	1.05×10^{2}	3.88×10^{16}	6.00×10^{1}
	5.44×10^{2}	3.64×10^{5}	8.41×10^{2}	6.02×10^{2}	6.80×10^{16}	1.22×10^{2}
	3.78	4.87				
	6.62	8.87				
	9.46	1.37×10^{1}				
	1.23×10^{1}	1.94×10^{1}				
	3.78×10^{1}	1.39×10^{2}				
HpMC(440)	9.46×10^{1}	1.15×10^{3}	1.82×10^{1}	1.61×10^{1}	6.84×10^{15}	1.50×10^{1}
	1.51×10^{2}	1.42×10^{3}	5.19×10^{1}	4.61×10^{1}	1.09×10^{16}	2.40×10^{1}
	2.27×10^{2}	2.45×10^{4}	1.49×10^{2}	1.36×10^{2}	1.64×10^{16}	3.70×10^{1}
	3.22×10^{2}	9.81×10^{3}	4.35×10^{2}	3.79×10^{2}	2.33×10^{16}	5.00×10^{1}
	3.78×10^{2}	1.80×10^{5}	6.49×10^{2}	6.43×10^{2}	2.74×10^{16}	6.70×10^{1}
	5.20×10^{2}	6.54×10^{5}	1.56×10^{3}	1.68×10^{3}	3.76×10^{16}	1.00×10^{2}
	6.62×10^{2}	1.72×10^{6}	3.24×10^{3}	3.29×10^{3}	4.79×10^{16}	1.20×10^{2}

Table SI6. Data for **Figure SI1** in this Supplementary Information for the original unfractionated HpMC sample

$\bar{L}^3\nu$	$\eta_{sp}N_A\bar{L}^3(M_w[\eta])^{-1}$	τ_w/τ_{r0}	$\bar{\tau}_r/\tau_{r0}$	ν/mL	J_e^{-1}/ Pa
9.76	1.70×10^{1}				
1.21×10^{1}	2.35×10^{1}				
1.39×10^{1}	2.89×10^{1}				
1.57×10^{1}	3.42×10^{1}				
9.96×10^{1}	1.23×10^{3}	6.33×10^{1}	1.67×10^{1}	1.08×10^{16}	7.00
1.99×10^{2}	1.01×10^{4}	3.07×10^{2}	7.24×10^{1}	2.15×10^{16}	1.25×10^{1}
2.99×10^{2}	4.47×10^{4}	9.04×10^{2}	1.93×10^{2}	3.23×10^{16}	1.70×10^{1}
3.98×10^{2}	1.52×10^{5}	1.45×10^{3}	4.77×10^{2}	4.30×10^{16}	3.50×10^{1}
5.97×10^{2}	6.56×10^{5}	4.34×10^{3}	1.44×10^{3}	6.45×10^{16}	5.30×10^{1}
7.96×10^{2}	2.59×10^{6}	1.45×10^{4}	4.09×10^{3}	8.60×10^{16}	6.00×10^{1}

References

SI1) Yoshida, M.; Arai, K.; Nakagawa, D.; Horikawa, Y.; Iwase, H.; Kumada, T.; Motokawa, R.; Shikata, T. Formation of Rod-Like Particles with Periodic Interior by Hydroxypropylmethyl Cellulose Samples with Narrow Molar Mass Distributions in Aqueous Solutions. *Biomacromolecules* **2025**, *26*, 8332-8342.

SI2) Doi, M.; Edwards, S. F.; *The Theory of Polymer Dynamics*. Clarendon Press: Oxford, **1986**; Chapter 8.

SI3) Doi, M.; S. F. Edwards, Dynamics of rod-like macromolecules in concentrated solution. Part 1. *J. Chem. Soc., Faraday Trans.* 2 **1978**, *74*, 560-570.

SI4) Ortega, A.; García de la Torre, J. Hydrodynamic properties of rodlike and disklike particles in dilute solution. *J. Chem. Phys.* **2003**, *119*, 9914-9919.

SI5) Hozumi, H.; Saiki, E.; Horikawa, Y.; Shikata, T. Rigid rod particle like viscoelastic responses of poly(vinylidene fluoride) in *N*-methylpyrrolidone solution. *J. Rheol.* **2023**, *67*, 683-692.

SI6) Hasegawa, H.; Horikawa,Y. and Shikata, Cellulose Nanocrystals as a Model Substance for Rigid Rod Particle Suspension Rheology, *Macromolecules* **2020**, *53*, 2677-2685.

SI7) Huggins, M. L. The viscosity of dilute solutions of long-chain molecules. IV. Dependence on concentration. *J. Am. Chem. Soc.* **1942**, *64*, 2716-2718.

SI8) Yoshida, M.; Hozumi, H.; Horikawa, Y.; Shikata, T. Viscoelastic Behavior of Aqueous Hydroxypropyl Cellulose Solutions Due to Entanglements. *Biomacromolecules* **2025**, *26*, 1294-1304.

SI9) Saiki, E.; Nakagawa, D.; Horikawa, Y.; Shikata, T. Rigid Rod-like Viscoelastic Behaviors of Methyl Cellulose Samples with a Wide Range of Molar Masses Dissolved in Aqueous Solutions. *Molecules* **2024**, *29*, 466.